

## Extensive relativistic-random-phase-approximation study of photoionization from atomic ytterbium

P. C. Deshmukh

*Department of Physics, Indian Institute of Technology, Madras 600 036, India*

S. T. Manson

*Department of Physics and Astronomy, Georgia State University, Atlanta, Georgia 30303*

(Received 4 August 1986)

Subshell photoionization parameters for photoionization from the  $4f$ ,  $5p$ , and  $5s$  subshells of atomic ytterbium have been calculated using the relativistic random-phase approximation (RRPA). Interference effects from interchannel coupling of 21 relativistic dipole channels have been included. Interesting differences in the results for  $4f$  parameters relative to a previous eight-channel RRPA calculation have been observed and are attributed to strong effects coming from coupling with the  $5p$  channels.

### I. INTRODUCTION

Recently, ESSR (electron spectroscopy using synchrotron radiation) measurements on atomic ytterbium were reported along with a theoretical calculation of the  $4f$  photoionization parameters using a truncated RRPA (relativistic random-phase approximation).<sup>1</sup> The following eight relativistic dipole channels were coupled in this RRPA calculation:

$$4f_{5/2} \rightarrow g_{7/2}, d_{5/2}, d_{3/2},$$

$$4f_{7/2} \rightarrow g_{9/2}, g_{7/2}, d_{5/2},$$

and

$$6s \rightarrow p_{3/2}, p_{1/2}.$$

A fairly satisfactory agreement between this eight-channel RRPA calculation and the ESSR data was found, in so far as  $4f$  cross section was concerned, after the relative experimental data were normalized to the theory at one energy point. There were some differences, however, in the experimental findings of the angular distribution asymmetry parameter and the results of the eight-channel RRPA calculation.<sup>1</sup> Around the same time that these results were reported, we had undertaken an extensive RRPA study of photoionization from atomic ytterbium in which in order to minimize possible errors due to truncation we included interchannel coupling from the following 21 relativistic dipole channels:

$$4d_{3/2} \rightarrow f_{5/2}, p_{3/2}, p_{1/2}, \quad 4d_{5/2} \rightarrow f_{7/2}, f_{5/2}, p_{3/2},$$

$$5s \rightarrow p_{3/2}, p_{1/2},$$

$$5p_{1/2} \rightarrow d_{3/2}, s, \quad 5p_{3/2} \rightarrow d_{5/2}, d_{3/2}, s,$$

$$4f_{5/2} \rightarrow g_{7/2}, d_{5/2}, d_{3/2}, \quad 4f_{7/2} \rightarrow g_{9/2}, g_{7/2}, d_{5/2},$$

and

$$6s \rightarrow p_{3/2}, p_{1/2}.$$

Coupling of such a large number of channels is computationally very demanding but has the advantage of minimizing the ambiguities that may arise from the exclusion of some of these channels.<sup>2</sup> The present calculations have been made up to a photon energy of 100 eV at which photoionization channels from the  $5p$  and  $5s$  shells are also open in addition to the eight-channels included in the previous study.<sup>1</sup> Photoionization parameters for ionization from the  $4f$ ,  $5p$ , and  $5s$  shells of atomic ytterbium are reported below. A detailed discussion of the RRPA method<sup>3</sup> and on some of its applications to some small<sup>4-6</sup> and some large<sup>7,8</sup> atoms can be found elsewhere.

### II. RESULTS AND DISCUSSION

For photon energies below the two spin-orbit split  $5p$  thresholds is a region where autoionization resonances occur. Experimental observations on these resonances have been reported<sup>9</sup> and the resonances have been partially analyzed theoretically<sup>1</sup> within the framework of the relativistic multichannel quantum-defect theory.<sup>10</sup> We have not in the present work included an analysis of these resonances and we report our findings only above the  $5p$  thresholds, where one would expect to see the effects of interchannel coupling between photoionization channels arising from the  $5p$  subshells and the  $4f$  subshells in particular. Furthermore, below these resonances, our results are in fair agreement with the eight-channel work, so this region is not discussed either.

In Fig. 1 is reported the partial photoionization cross section from the two  $4f$  subshells. In the same figure are shown the results of the relative ESSR measurements and the previous eight-channel RRPA calculations.<sup>1</sup> As is well known,<sup>11</sup> calculations of photoionization cross sections made in the length and the velocity form agree with each other in the full RRPA, but differences between the two appear as a result of truncation. Hence one observes two distinct curves in the results of the previous eight-channel study. In the present work, since almost all of the important dipole channels were coupled, the agreement

between the length and the velocity forms is almost perfect and hence only a single curve is drawn in Fig. 1 for the cross section. The general shape of the total cross section as determined in the present work is almost identical, nevertheless, to the shape of the eight-channel result, but the present calculation shows a mild flattening of the curve at the higher energy which is perhaps consistent with the shape of the experimental data. The present results are, however, significantly larger than the cross section calculated in the eight-channel RRP. The main effect of interchannel coupling with photoionization from the  $5p$  subshells on  $4f$  photoionization is, therefore, an overall increase in the  $4f$  cross section. This effect is significant and needs to be included despite the fact that there are only six electrons in the  $5p$  shell as opposed to fourteen in the  $4f$ . This is true even though the *total* oscillator strength from the  $4f$  subshells is more than double the  $5p$ . The existence of a huge centrifugal barrier in the final state of the principal source of  $4f$  oscillator strength,  $f$ - $g$  transitions, means that the  $4f$  cross section is small at threshold and rises very slowly to a broad, and not very high maximum; this rise is illustrated in Fig. 1. The  $5p$  subshell, on the other hand, does not have this huge a potential barrier in the main  $p$ - $d$  transitions, so its oscillator strength is concentrated near the  $5p$  thresholds. Just above the  $5p$  thresholds, the cross section from the two  $5p$  subshells is nearly four and a half times that from the  $4f$ , as seen in Fig. 2. In fact, the  $5p$  cross section is higher than the  $4f$  cross section till photon energy of  $\sim 50$  eV, above which it becomes weaker rapidly, as can be seen from Fig. 2. The influence of  $5p$  photoionization on that from  $4f$ , therefore, gradually becomes weaker at higher energies, at which one does find the present 21-channel

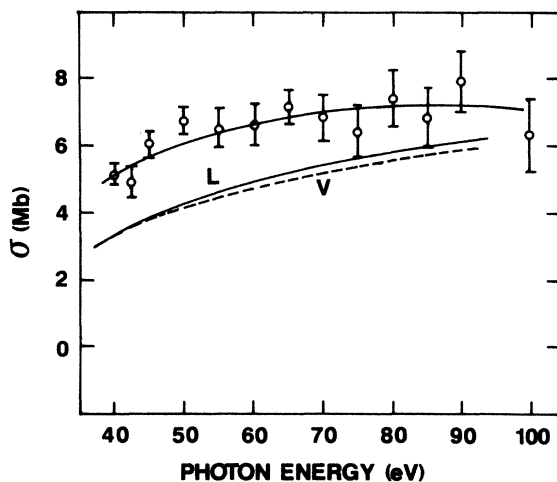


FIG. 1. Photoionization cross section for the  $4f$  subshell. The upper continuous solid curve represents the results of the present investigation in which 21 dipole channels were coupled. The lower continuous and the dashed curve represents the length and velocity forms of the previous eight-channel RRP study of Ref. 1. The experimental data points of Ref. 1 have been lifted upwards in this figure to renormalize the measured relative cross section to the present result at 40 eV.

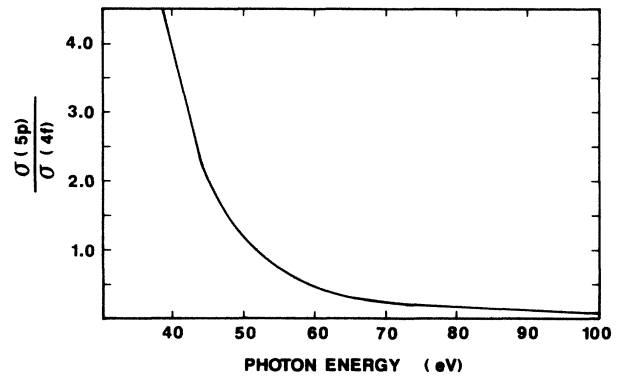


FIG. 2. Branching ratio of Yb  $5p$  cross section relative to the  $4f$  cross section. The relatively high value of this ratio just above the  $5p$  thresholds, remaining greater than 1 until photon energy of  $\sim 52$  eV is an indicator of the importance of coupling  $5p$  channels to those from  $4f$ .

calculations to come in closer agreement with the previous eight-channel calculations than at lower photon energies. The present results should be more reliable since they include the influence of interchannel coupling with ionization from the  $5p$  which seems to be significant. It should be emphasized that the experimental data of Ref. 1 were normalized to our result at an arbitrarily chosen point at the photon energy of 40 eV in the absence of an absolute measurement, similar to what was done previously with the eight-channel result.

The branching ratio for photoionization from the  $4f_{7/2}$  subshell relative to that from the  $4f_{5/2}$  subshell, however, is almost unaltered in the present calculation from the previous eight-channel calculation and is therefore not presented in this paper. This means that the strengths of photoionization channels from the  $4f_{7/2}$  and  $4f_{5/2}$  increase by the same factor due to coupling with  $5p$  channels.

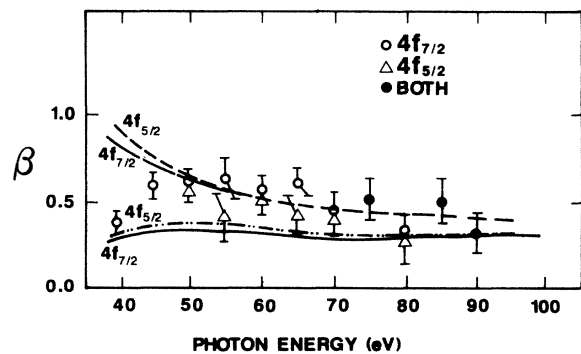


FIG. 3. Angular distribution asymmetry parameter for  $4f_{7/2}$  and  $4f_{5/2}$  photoionization (lower curves). Also shown with the present 21-channel results are the results of previous eight-channel study (upper curves) and the experimental data of Ref. 1.

The photoelectron angular distribution asymmetry parameter  $\beta$  depends upon the ratios of the matrix elements of the various photoionizing channels (essentially the branching ratios) along with their relative phases. The additional channels were seen to leave the branching ratios unaffected. The effect of the interchannel coupling of  $5p$  with  $4f$  does, however, change  $\beta$  considerably, as seen in Fig. 3. Thus, it is clear that this coupling does affect the phase shifts appreciably. In Fig. 3 are shown, along with the present 21-channel results, the results for the angular distribution asymmetry parameter of the previous eight-channel calculations as well as the experimental data.<sup>1</sup> The largest discrepancy between the present 21-channel calculation and the previous eight-channel calculation occurs just above the  $5p_{1/2}$  thresholds, where as mentioned earlier, the oscillator strength from the  $5p$  subshells is large relative to  $4f$ . The experimental datum at 40 eV, just above the  $5p_{1/2}$  threshold, is in very good agreement with the present calculation, whereas the previous eight-channel calculation gives a much higher value for the asymmetry parameter at that energy. At higher photon energies, it is difficult to say whether the eight-channel or the 21-channel calculation agrees better with the experimental data, but we trust that the present results being more complete ought to be more reliable and are certainly in fair agreement with the experimental data, within the limits of experimental accuracy. As in the case of  $4f$  cross section, the results for the angular distribution asymmetry parameter in the eight-channel calculation and the 21-channel calculation again come closer at higher photon energies as photoionization from  $5p$  gets weaker.

In Fig. 4 is shown the sum of the photoionization cross sections from the  $5p_{3/2}$  and the  $5p_{1/2}$  subshells. As is seen in Fig. 4,  $5p$  photoionization is pretty strong above the thresholds but decreases monotonically as photon energy increases. As mentioned before, this energy dependence is responsible for influencing  $4f$  photoionization pa-

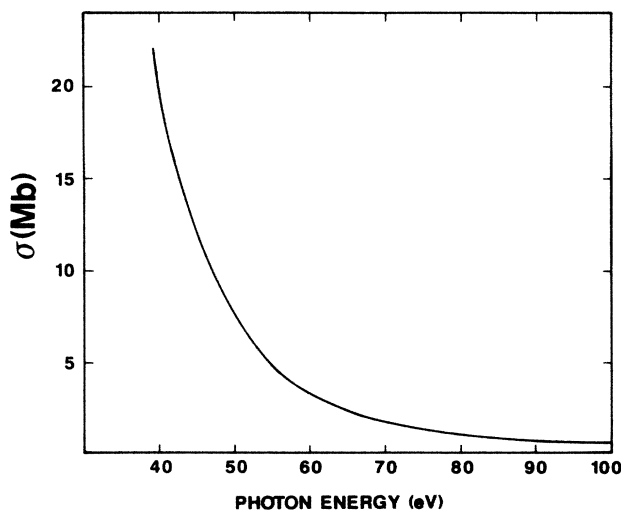


FIG. 4. Photoionization cross section for the  $5p$  subshell. The curve represents the sum of the cross sections from the  $5p_{3/2}$  and  $5p_{1/2}$  spin-orbit split doublet levels.

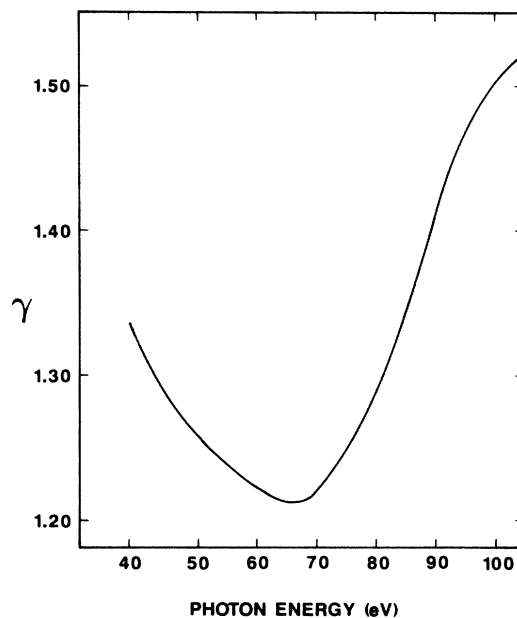


FIG. 5. The branching ratio for photoionization from the  $5p_{3/2}$  relative to that from the  $5p_{1/2}$  subshells. This interesting profile is an indicator of the qualitative positions of the Cooper minima in the dominant photoionization channels.

rameters significantly near the two  $5p$  thresholds, but this influence gets rapidly weaker as photon energy increases.

The branching ratio for photoionization from the  $5p_{3/2}$  subshell relative to that from the  $5p_{1/2}$  subshell is shown in Fig. 5. Over the entire energy region considered here,

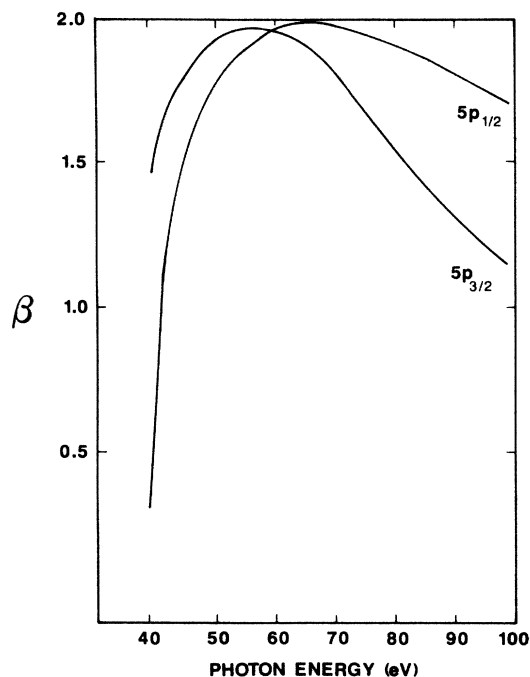


FIG. 6. The angular distribution asymmetry parameter for photoionization from the  $5p_{3/2}$  and  $5p_{1/2}$  subshells.

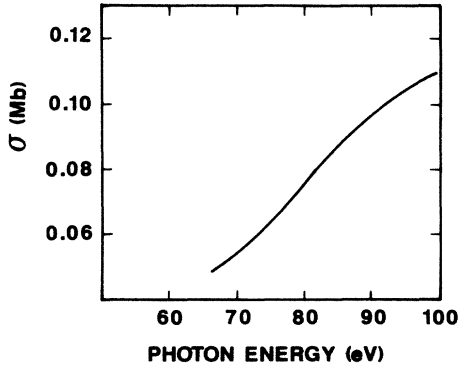


FIG. 7. The  $5s$  subshell cross section. This figure suggests that the  $5s$  Cooper minimum is in the discrete spectrum.

the branching ratio is considerably below the statistical value of 2. In fact, from a value of 1.335 above the  $5p_{1/2}$  thresholds, it first decreases further till the photon energy is  $\sim 67$  eV above which it starts increasing. One has to remember here that especially above photon energy of  $\sim 52$  eV, interchannel coupling with the  $4f$  channels should become a significant factor to be considered in influencing  $5p$  parameters and will manifest itself in the  $5p$  branching ratio also.

The general behavior of the branching ratio, well below statistical near threshold and rising rapidly above the region, has a relatively simple explanation. Both  $5p_{3/2}$  and  $5p_{1/2}$  have Cooper minima in the dominant  $p-d$  channels, but above the energies we have considered. Nevertheless, it is known<sup>12</sup> that the zeros for the  $5p_{3/2}-d$  transitions occur at energies well below the  $5p_{1/2}-d$ . Each cross section has the general behavior of dropping rapidly from threshold (where  $p-d$  channels dominate) followed by a much slower dropoff where the  $p-s$  channels are largest. Since the  $5p_{3/2}$  does this at lower energies, a drop in the branching ratio from its threshold value is seen. Then, when the  $5p_{3/2}$  is predominantly  $p-s$ , the  $5p_{1/2}$  is still mostly  $p-d$  and dropping rapidly, causing the subsequent rise in the branching ratio. This rise is expected to continue to a value well above statistical at higher energies as was seen for the  $6p$  in a number of elements.<sup>12</sup>

The angular distribution asymmetry parameter  $\beta$  for photoionization from the  $5p$  subshells is shown in Fig. 6. Couplings between  $j-j$  and  $j-(j\pm 1)$  channels result in strong energy dependence of the  $5p_{3/2}$  and  $5p_{1/2}$  asymmetry parameters, which are different from each other. After the initial rise to  $\beta \sim 2$ , the angular distribution asymmetry parameter for the  $5p_{3/2}$  subshell falls relatively more sharply than that for the  $5p_{1/2}$  subshell confirming that the Cooper minimum in the  $p-d$  channels occur

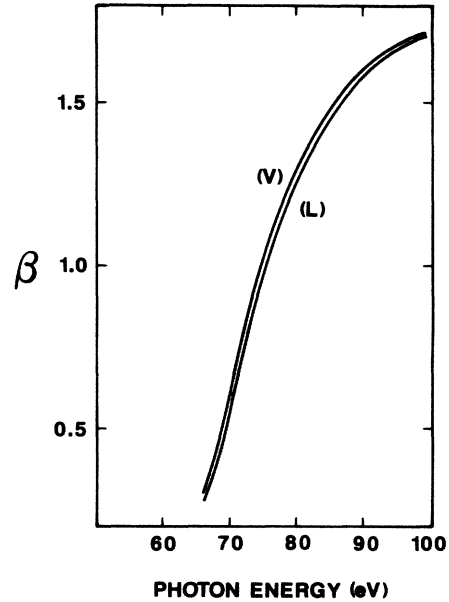


FIG. 8. The  $5s$  angular distribution asymmetry parameter.

at a lower energy for the  $5p_{3/2}$  subshell than for the  $5p_{1/2}$  subshell.<sup>13</sup> The fact that the parameter  $\beta$  for  $5p_{3/2}$  is higher than that for  $5p_{1/2}$  near the threshold, but at  $\sim 58.5$  eV this order is reversed, is similar to photoionization from the  $5p$  subshells of xenon.<sup>11</sup>

The cross section for  $5s$  photoionization is shown in Fig. 7 where a rather significant rise from threshold is seen. This is rather uncharacteristic of an  $ns$  cross section; it looks rather like a "recovery" from a Cooper minimum which, in this case, appears to lie in the discrete (autoionizing) region just below threshold. If this is true, it should also be reflected in a value of  $\beta$  near threshold which is significantly different from 2. Looking at Fig. 8, which shows the  $\beta$  parameter, a rather dramatic departure of  $\beta$  from 2 is evident. This confirms a Cooper minimum in the  $5s-p$  channels just below threshold, similar to the case of Al  $3s$  photoionization.<sup>14,15</sup> An analysis of the  $5s-np$  autoionizing states should confirm this fact.

#### ACKNOWLEDGMENTS

The present calculations have been made using the computer codes written by W. R. Johnson, University of Notre Dame. We are thankful to him for his help in the present investigation. This work was supported by the U.S. Army Research Office.

<sup>1</sup>W. A. Svensson, M. O. Krause, T. A. Carlson, V. Radojević, and W. R. Johnson, Phys. Rev. A 33, 1024 (1986).

<sup>2</sup>P. C. Deshmukh and S. T. Manson, Phys. Rev. A 32, 3109 (1985).

<sup>3</sup>W. R. Johnson and C. D. Lin, Phys. Rev. A 20 964 (1979).

<sup>4</sup>W. R. Johnson and K. T. Cheng, Phys. Rev. A 20, 978 (1979).

<sup>5</sup>P. C. Deshmukh and W. R. Johnson, Phys. Rev. A 27, 326

(1983).

<sup>6</sup>P. C. Deshmukh and S. T. Manson, A 28, 209 (1983).

<sup>7</sup>W. R. Johnson and V. Radojević, Phys. Lett. 92A, 75 (1982).

<sup>8</sup>P. C. Deshmukh, B. R. Tambe, and S. T. Manson, Aust. J. Phys. (to be published).

<sup>9</sup>D. H. Tracy, Proc. R. Soc. London, Ser. A 357, 485 (1977).

<sup>10</sup>C. M. Lee and W. R. Johnson, Phys. Rev. A 10, 1598 (1980).

<sup>11</sup>W. R. Johnson, C. D. Lin, K. T. Cheng, and C. M. Lee, Phys. Scr. **21**, 409 (1980).

<sup>12</sup>S. T. Manson, C. J. Lee, R. H. Pratt, J. B. Goldberg, B. R. Tambe, and A. Ron, Phys. Rev. A **28**, 2885 (1983).

<sup>13</sup>P. C. Deshmukh, V. Radojević, and S. T. Manson (unpublish-

ed).

<sup>14</sup>S. Shahabi, Phys. Lett. A **72**, 212 (1979).

<sup>15</sup>S. T. Manson and A. F. Starace, Rev. Mod. Phys. **54**, 389 (1982).